# G70.7+1.2: A nonthermal bubble in a globule - Nova, supernova remnant, or outflow?

Bally, J.; Pound, M.W.; Stark, A.A.; Israel, F.P.; Hirano, N.; Kameya, O.; ... ; Hereld, M.

THE ASTROPHYSICAL JOURNAL, 338:L65–L68, 1989 March 15


# G70.7+1.2: A NONTHERMAL BUBBLE IN A GLOBULE—NOVA, SUPERNOVA REMNANT, OR OUTFLOW?

JOHN BALLY,[1] MARC W. POUND,[1] ANTONY A. STARK,[1] FRANK ISRAEL,[2] NAOMI HIRANO,[3] OSAMU KAMEYA,[3] KAZUYOSHI SUNADA,[4] MASAHIKO HAYASHI,[4] HARLEY THRONSON, JR.,[5] AND MARK HERELD[6]

*Received 1988 September 9; accepted 1988 December 21*

## ABSTRACT

We present millimeter-wave, near-infrared, and 21 cm observations of the radio source G70.7+1.2 which has been proposed to be a recent supernova remnant developing inside a molecular cloud. The distance to this object is found to be $4.5 \pm 1$ kpc. A small molecular cloud with properties similar to a large dark cloud or globule is interacting with the nonthermal radio continuum source. The molecular cloud has a lumpy structure with its highest column density portion lying just outside the brightest portion of the radio continuum shell. If the radio source was produced by a supernova explosion, its kinetic energy was several orders of magnitude less than that of most observed supernovae. The energy produced by an OB star wind with $\dot{M}_* = 10^{-6}\ M_\odot\ \mathrm{yr}^{-1}$ at $V_w = 10^3$ km s$^{-1}$ is sufficient to drive the bubble. However, the high radio continuum nonthermal surface brightness and polarization of G70.7+1.2 is not explained by this model. The physical nature of this source remains mysterious. G70.7+1.2 contains a unique combination of a molecular cloud and a nonthermal radio source and may provide an opportunity to investigate relativistic particle acceleration and injection.

*Subject headings:* infrared: sources — interstellar: molecules — nebulae: supernova remnants — radio sources: general

## I. INTRODUCTION

The compact Galactic radio source G70.7+1.2 was classified as a supernova remnant by Reich *et al.* (1984) based on its nonthermal spectrum between 408 MHz and 22 GHz, its shell-like structure approximately 20″ in diameter, and its polarization. The exceptionally high surface brightness and compact size prompted Reich *et al.* (1985) to suggest that this remnant is only a little over 100 yr old and produced by a supernova which exploded inside a molecular cloud. An optical nebula coincident with G70.7+1.2 (Minkowski 1948) was found by de Muizon *et al.* (1988) to have a spectrum indicating shock excitation in a moderate density ($n \approx 10^3$ cm$^{-3}$) medium and a shock velocity of order 100–200 km s$^{-1}$, much lower than might be expected for such a young supernova. A search with *EXOSAT* failed to detect X-ray emission from this source. De Muizon *et al.* (1988) note that G70.7+1.2 coincides with a bright compact *IRAS* source in Cygnus having a 100 $\mu$m flux of nearly 400 Jy and a spectrum like a young stellar object. Analysis of the 8–22 $\mu$m *IRAS* Low-Resolution Spectrometer spectra shows that the *IRAS* source exhibits 7.7, 8.6, and 11.3 $\mu$m emission usually attributed to polycyclic aromatic hydrocarbons. A highly reddened pointlike infrared source (6th mag at 2.2 $\mu$m and fainter than 18th in the visual) lies near the center of the radio shell. Recently, Becker and Fesen (1988) obtained more optical spectroscopy and narrow-band CCD imagery. They argue that G70.7+1.2 is similar in nature to the Herbig-Haro objects frequently found to be associated with energetic outflows from young stellar objects (Bally and Lada 1983; Lada 1985). The nonthermal nature of G70.7+1.2 has been unambiguously demonstrated by a recent measurement of the 89 GHz continuum flux by Balonek and Dent (1988) who find that $S_{89} < 80$ mJy, nearly 10 times less than the value expected from a thermal source. Clearly, G70.7+1.2 is unusual; it exhibits characteristics of both supernova remnants and outflow sources associated with pre–main-sequence stars. We present new millimeter-wave molecular observations, near-infrared array camera images, and 21 cm H I spectra of the environment of G70.7+1.2.

[1] AT&T Bell Laboratories, Crawford Hill.
[2] Sterrewacht, Leiden.
[3] Nobeyama Radio Observatory, Japan.
[4] Department of Astronomy, University of Tokyo.
[5] Wyoming Infrared Observatory, University of Wyoming.
[6] Department of Astronomy and Astrophysics, University of Chicago.

## II. OBSERVATIONS AND DATA REDUCTION

### a) *Bell Laboratories*

We used the 7 m offset Cassegrain telescope located on Crawford Hill in Holmdel, New Jersey to obtain observations of the 110 GHz $^{13}$CO, the 115 GHz $^{12}$CO, and 98 GHz CS transitions. At these frequencies, this antenna has a very clean Gaussian beam 100″ in diameter. Details of the observing and reduction techniques are described in Bally *et al.* (1987). An isolated group of three small molecular clouds was discovered in the CO line with the brightest component centered at $V_{\mathrm{LSR}} \approx 5$ km s$^{-1}$. Two small, weak, $^{12}$CO emitting clouds are centered at $V_{\mathrm{LSR}} \approx 9$ km s$^{-1}$ and located at (5, 1) and (−3, 0) in arcminute offsets (see Fig. 1 [Pl. L5]). The 5 km s$^{-1}$ cloud is approximately centered on the radio continuum source and has a peak brightness temperature of 10 K. As shown in Figure 1*b*, the $^{12}$CO emission shows faint line wings at the 50 mK level extending from $V_{\mathrm{LSR}} = -15$ to 10 km s$^{-1}$ similar to those seen in the high-velocity molecular outflows from young stellar objects or older supernova shock waves interacting with molecular gas (e.g., IC 443; de Noyer 1979). A 1 K background cloud at $V_{\mathrm{LSR}} \approx -62$ km s$^{-1}$ is also observed in $^{12}$CO. We failed to detect the 98 GHz $J = 2$–1 line of CS at a level of 50 mK, indicating that there is little molecular gas at densities above $10^3$ cm$^{-3}$.

*b) Nobeyama Radio Observatory*

The 45 m telescope at the Nobeyama Radio Observatory (NRO) in Japan was used to obtain 15″ resolution maps of $^{12}$CO and $^{13}$CO emission from the core of G70.7 + 1.2 (see Figs 2 [Pl. L6] and 3 [Pl. L7]). A Bell Laboratories SIS receiver ($T_{SSB} \approx 200$ K) was used in addition to the 3 mm Millitech receiver ($T_{SSB} \approx 350$ K) under poor weather conditions in early 1988 June to map the inner 2′ portion of the molecular cloud. The high-resolution $^{13}$CO maps show lumpy structure and a peak in both line temperature and integrated intensity just to the northeast of the radio shell where the continuum emission exhibits the highest surface brightness. The $^{12}$CO emission peaks near this position and shows an arc of emission which surrounds the northern edge of the radio continuum shell. The CO emission and the radio continuum shell exhibit complementary morphologies, leaving little doubt that the nonthermal plasma and molecular gas are interacting. We failed to detect $HCO^+$ emission at the 0.2 K level. We also searched for the $v = 1$–0, $J = 1$–0 SiO maser line at 43 GHz which is frequently found in oxygen-rich late-type stars. We saw no emission at the 1 K level.

*c) Wyoming Infrared Observatory*

Near-infrared images in the $H$ (1.6 $\mu$m; Fig. 3) and $K$ (2.2 $\mu$m; Fig. 2) bands were obtained with the 2.3 m Cassegrain telescope at the Wyoming Infrared Observatory (WIRO) using the Astrophysical Research Consortium prototype near-infrared camera (Hereld, Harper, and Pernic 1989); the camera incorporates a Rockwell 64 × 64 pixel HgCdTe detector array. The infrared images show three components: a bright central star; a bright ridge about 6″ to the northeast which coincides with the peak radio emission and is close to the $^{13}$CO peak; and finally, an extended, filamentary nebulosity about 20″ in diameter.

*d) Westerbork*

The 21 cm line of atomic hydrogen was observed with the Westerbork Synthesis Array (WSRT). The H I line can be seen in absorption against the radio continuum shell up to $V_{LSR} \approx 29$ km s$^{-1}$.

## III. SOURCE PROPERTIES

In the direction of G70.7 + 1.2, we see H I emission between 24 km s$^{-1}$, which arises at the tangent point, the point along the line of sight nearest to the Galactic center, and −87 km s$^{-1}$, which arises at a point 15.5 kpc distant, according to the Galactic rotation curve of Brand (1986). H I absorption is seen between $V_{LSR} = 29$ to −6.5 km s$^{-1}$ (Fig. 1*d*). Absorption at 29 km s$^{-1}$ implies that G70.7 + 1.2 is farther from us than the tangent point, farther than 1.5 kpc. Absence of absorption at large negative velocities implies that G70.7 + 1.2 is closer than 6 kpc. The kinematic distance of the −62 km s$^{-1}$ CO feature is ≈12 kpc, placing this cloud in the outer Galaxy beyond the solar circle.

We also estimate the distance using the correlation of the CO line width with the physical size of clouds (Meyers 1983; Solomon *et al.* 1986). Using the $^{13}$CO maps of the Orion cloud from Bally *et al.* (1987) and the first-quadrant Bell Laboratories $^{13}$CO survey to calibrate a relation between physical radius $R$ and the FWHM line width, which has the form $\log(\Delta V) = m[\log(R)] + b$, we obtain a distance

$$D = \frac{1}{\theta_{1/2}} \text{ dex} \left\{ \frac{\log [\Delta V(\text{FWHM})] - b}{m} \right\} \text{(pc)} ,$$

where $\theta_{1/2}$ is the angular radius of the cloud in radians, and $\Delta V$ is in km s$^{-1}$. Table 1 summarizes the various values of the coefficients $m$ and $b$ found by different groups and the distance to G70.7 + 1.2 that each yields. These estimates indicate that G70.7 + 1.2 is most likely to lie at a distance of 4.5 ± 1 kpc, in good agreement with the H I constraints.

Assuming $^{12}$CO to be optically thick and thermalized, we estimate that the average excitation temperature of the CO 1–0 transition is about 13 K. This is typical of cold dark clouds and globules and unlike the core of a giant molecular cloud where massive star formation has taken place. Our failure to detect CS and $HCO^+$ emission indicates that there is no dense cloud core in G70.7 + 1.2. Thus, even in the presence of the luminous *IRAS* source, the gas is not likely to be heated by collisions with hot dust grains.

We estimate the cloud mass by assuming that the $^{13}$CO emission is optically thin and thermalized, and that $N(H_2)/N(^{13}CO) = 7 \times 10^5$ (Frerking, Langer, and Wilson 1982). Thus, the $H_2$ mass is given by

$$M(H_2) = 1.3\ m(H_2) \int N(H_2) dA ,$$

where

$$N(H_2) = 1.5 \times 10^{20} \int T_A^*(^{13}CO) dV/\eta [1 - e^{(5.29K/T_{ex})}] .$$

Integrating the Bell Laboratories $^{13}$CO map over all three components gives a total mass of $\sim 1 \times 10^3 D_{4.5}^2\ M_\odot$, where $D_{4.5}$ is the distance in units of 4.5 kpc. The two fainter components contain about 5% and 10% of this mass, respectively. The molecular cloud is about $3D_{4.5}$ pc in diameter, typical of large globules or dark clouds and much smaller than a giant molecular cloud. Assuming the cloud is spherical with a diameter of 3 pc, the mean density of the molecular gas is $10^3$

TABLE 1

DERIVED DISTANCE PARAMETERS FOR G70.7 + 1.2[a]

| Source | Number of Clouds in Sample | $m$ | $b$ | $D$ (kpc) | Comments |
|---|---|---|---|---|---|
| Myers 1983 | 43 | 0.5 | 0.03 | 6.1 | |
| Bally *et al.* 1987 | 12 | 0.71 | 0.41 | 3.8 | $\theta_{1/2} = (\text{area}/\pi)^{1/2}$. |
| AT&T BL $^{13}$CO survey | 25 | 0.65 | −0.04 | 5.3 | $\theta_{1/2} = (\theta_l \theta_b)^{1/2}$; unweighted fit. |
| | 25 | 0.71 | −0.09 | 5.6 | Weighted by $\{\sigma[\Delta V(\text{FWHM})]/\Delta V(\text{FWHM})\}$. |
| Stark 1979 | 106 | 0.36 | 0.15 | 4.0 | Weighted as above; cloud diameters rounded to nearest 5 pc. |
| Solomon *et al.* 1986 | 250 | 0.5 | 0.15 | 2.5 | Using $^{12}$CO line width and cloud size. |

[a] Distance given by the relation $D = (1/\theta_{1/2})$ dex $\{\log [\Delta V(\text{FWHM})] - b\}/m$ (pc).

$cm^{-3}$, which is consistent with our failure to detect any high dipole moment molecules.

## IV. THE NATURE OF G70.7+1.2

The optical spectroscopy of G70.7+1.2 has constrained the shock velocity in the expanding shell of G70.7+1.2 to $V_s < 200$ km $s^{-1}$, while the molecular observations constrain the density of the ambient medium to $n(H_2) \approx 10^3$ $cm^{-3}$. A distance of 5 kpc implies the radio shell is about 0.5 pc in diameter, with a radio luminosity of $L_R = 0.2$ $L_\odot$, and a far-infrared luminosity of $L_{IR} = 3 \times 10^4$ $L_\odot$. If the shell was produced by a supernova still in the free expansion phase ($M_{shell} < M_{ejecta}$), the expansion velocity of the blast wave should be much greater than $10^3$ km $s^{-1}$. The optical velocities and constraints derived from line strength and excitation arguments indicate that this is not the case; the shell must be either in the adiabatic (nonradiative) or momentum conserving (radiative) state. The Sedov (1959) solution for a point explosion implies $V_s = 10^3 r_{18}{}^{-1.5}[E_{50}/n_3]^{0.5}$(km $s^{-1}$), in the adiabatic case, and $V_s = 2 \times 10^3 r_{18}{}^{-3}[E_{50}\ M_\odot]^{0.5}/n_3$(km $s^{-1}$), in the momentum conserving case, where $E_{50}$ is the explosion energy in units of $10^{50}$ ergs, $r_{18}$ is the radius of the shock in units of $10^{18}$ cm, $n_3$ is the ambient density in units of $10^3$ $cm^{-3}$, and $M_\odot$ is the ejected mass in solar units. Thus for a $10^{50}$ ergs explosion and a shell radius and ambient density like those found in G70.7+1.2, we expect a shock velocity in excess of $10^3$ km $s^{-1}$. The energy injected into the expanding shell must therefore be less than the kinetic energy of a typical supernova explosion by several orders of magnitude.

A supernova origin has the further difficulty that the molecular cloud has survived, intact, the entire presupernova, main-sequence phase. Neither a powerful stellar wind nor significant ionizing flux could have existed since this rather small cloud has not been disrupted. The absence of ionization implies a spectral type later than B2, but this makes the main-sequence life much longer than $10^7$ yr during which low-mass star formation and winds should have dispersed the cloud. Furthermore, a highly reddened luminous stellar object still exists inside the radio shell and has a spectrum similar to a Be star. The time spent by the stellar system inside the molecular cloud has an upper bound set by the radiative cloud disruption time scale which may be estimated from $t_{rad} \sim 3M_{cloud}\, c\Delta V_{CO}/2L \approx 3 \times 10^6$ to $3 \times 10^7$ yr. These arguments indicate that if the formation of the G70.7+1.2 radio shell involved a supernova event, the progenitor was not born in the associated molecular cloud, but has wandered into it by accident.

Several "exotic" scenarios for the origin of the nonthermal bubble are worth mentioning. The embedded star may be the remnant of a binary system in which one member underwent an unusually weak supernova explosion producing the nonthermal shell. It is also possible a binary system still exists consisting of the star and an invisible compact (neutron star) companion. Accretion of matter from the visible star onto the compact object may drive an ultrafast wind which might energize the nonthermal shell. In this latter model, there is a chance that the accreting companion may be either a radio or X-ray pulsar. Bondi-Hoyle accretion of cloud gas onto a compact object, such as a white dwarf near the Chandrasekhar limit, which happens to pass through the cloud at a low relative velocity may provide a natural trigger for an explosion under some circumstances. For a neutron star moving through a cloud at 1 km $s^{-1}$ the Bondi-Hoyle accretion luminosity is $\approx 2 \times 10^4$ $L_\odot$, comparable to the total infrared luminosity of G70.7+1.2. So, energetically, a "wind" produced by Bondi-Hoyle accretion onto an old neutron star could drive the nonthermal bubble.

A nova which releases $10^{45}$ ergs may satisfy the energetic requirements of G70.7+1.2 and is more likely to occur than a supernova in any particular volume by a factor of roughly $10^3$ ($R_{SN} \approx 0.02$ $yr^{-1}$ and $R_N \approx 40$ $yr^{-1}$; Allen 1973). For a molecular cloud volume filling factor in the Milky Way of 0.1% (Solomon *et al.* 1986, and references therein), a nova is expected to explode inside a molecular cloud somewhere in the Galaxy once every 25 yr or so, while a supernova is expected to occur only once every $5 \times 10^4$ yr. The spatial correlation between cloud complexes and supernova progenitors may decrease this rate by 10. However, the infrared luminosity of this object is much greater than any known quiescent-phase nova, probably ruling out this interpretation.

De Muizon *et al.* (1988) discuss the possibility that G70.7+1.2 is a post–main-sequence (PMS) star in the process of becoming a planetary nebula. We find little evidence for either an oxygen-rich or carbon-rich object. In the former case, SiO maser emission is expected, but we failed to find it. In the latter case, the CO emission from the expanding stellar envelope usually produces line widths greater than 20 km $s^{-1}$, but the observed CO lines show no such structure. Furthermore, the *IRAS* infrared colors resemble an embedded source, unlike a PMS star. These arguments may not, however, apply to a PMS object ejecting mass inside an unrelated molecular cloud.

Becker and Fesen (1988) suggest that this source is a young stellar object. This scenario incorporates in a natural way the presence of the molecular cloud, a stellar object, an infrared source, and shock-excited emission. High-mass stars can occasionally form in small clouds; S106 (Bally, Snell, and Predmore 1983) is an example. Energy-conserving and momentum-conserving wind bubbles (Castor, McRay, and Weaver 1977) produce shocks with a velocity $V_S = (\dot{M}_* V_W{}^2/4\pi n_0 m_H)^{1/3} r^{-2/3} \approx 200$ km $s^{-1}$ and $V_S = (\dot{M}_* V_W/4\pi n_0 m_H)^{1/2} r^{-1} \approx 100$ km $s^{-1}$, respectively, where $\dot{M}_* = 10^{-6}$ $M_\odot$ $yr^{-1}$, $V_W = 10^3$ km $s^{-1}$, $n_0 = 10^3$ nucleons $cm^{-3}$, and $r = 7 \times 10^{17}$ cm. Although energetically likely and physically plausible, the stellar wind hypothesis again requires that the star not have sufficient ionizing flux to damage the cloud. This, however, may be naturally satisfied if the stellar wind mass-loss rate exceeds a critical rate where the recombination rate is much greater than the ionization rate in the wind (S106 may be close to this critical mass loss rate; see Bally and Scoville 1982 and Felli *et al.* 1984). Although this model readily explains the presence of a molecular cloud and a shock-excited nebula, it does not explain the strong radio continuum nor its polarization. It is possible that supermassive stellar winds ramming dense gas naturally produce nonthermal radiation. This situation must be exceedingly rare, however: most OB stellar winds interact with lower density media or are much less powerful. The $10^3$ km $s^{-1}$ velocity hypothesized here is considerably greater than in most outflows from young stellar objects. It is interesting to note, however, that the highest velocity Herbig-Haro objects such as HH 1 and HH 2, and GGD 37 in Cepheus A are associated with radio continuum emission, although only at a mJy level. Perhaps G70.7+1.2 is one of the rare examples where a very fast wind from a young stellar object is producing strong nonthermal emission. This source may provide a readily studied example of the production of nonthermal radio emission in shocks.

We thank R. E. Miller for supplying the SIS junctions that made the millimeter-wave observations at both Bell Laboratories and at Nobeyama possible, the staff at NRO for their extensive help and hospitality, and Mike Jura for showing us a simple expression for the radiative disruption time scale. We thank Tom Balonek and William Dent for obtaining a measurement of the 89 GHz continuum flux density using the NRAO 12 m radio telescope on 1988 November 22.

REFERENCES

Allen, C. W. 1973, *Astrophysical Quantities* (London: Athlone).
Bally, J., and Lada, C. 1983, *Ap. J.*, **265**, 824.
Bally, J., Langer, W. D., Stark, A. A., and Wilson, R. W. 1987, *Ap. J.* (*Letters*), **312**, L45.
Bally, J., and Scoville, N. 1982, *Ap. J.*, **255**, 497.
Bally, J., Snell, R. L., and Predmore, R. 1983, *Ap. J.*, **272**, 154.
Bally, J., Stark, A. A., Wilson, R. W., and Henkel, C. 1988, *Ap. J.*, **324**, 223.
Balonek, T., and Dent, W. 1988, private communication.
Becker, R. H., and Fesen, R. A. 1988, *Ap. J.* (*Letters*), **334**, L35.
Brand, J. 1986, Ph.D. thesis, Leiden University.
Castor, J., MacCray, R., and Weaver, R. 1975, *Ap. J.* (*Letters*), **200**, L107.
de Muizon, M., Strom, R. G., Oort, M. J. A., Class, J. J., and Braun, R. 1988, *Astr. Ap.*, **193**, 248.
de Noyer, L. 1979, *Ap. J.* (*Letters*), **232**, L165.
Felli, M., Staude, H. J., Reddmann, T., Massi, M., Eiroa, C., Hefele, H., Neckel, T., and Panagia, N. 1984, *Astr. Ap.*, **135**, 261.
Frerking, M. A., Langer, W. D., and Wilson, R. W. 1982, *Ap. J.*, **262**, 590.
Hereld, M., Harper, D. A., and Pernic, R. 1989, in preparation.
Lada, C. J. 1985, *Ann. Rev. Astr. Ap.*, **23**, 267.
Myers, P. C. 1983, *Ap. J.*, **270**, 105.
Minkowski, R. 1948, *Pub. A.S.P.*, **60**, 386.
Reich, W., Furst, E., Altenhoff, W. J., Reich, P., and Junkes, N. 1985, *Astr. Ap.*, **151**, L10.
Reich, W., Furst, E., Stuffen, P., Reif, K., and Haslam, C. G. T. 1984, *Astr. Ap. Suppl.*, **58**, 197.
Sedov, L. I. 1959, *Similarity and Dimensional Methods in Mechanics* (Cambridge: Academic Press).
Solomon, P. M., Rivolo, A. R., Mooney, T. J., Barrett, J. W., and Sage, L. J. 1986, in *Star Formation in Galaxies*, ed. C. J. Lonsdale Persson (NASA CP-2466) (Washington: NASA), p. 37.
Stark, A. A. 1979, Ph.D. thesis, Princeton University.

JOHN BALLY: HOH L-245, AT&T Bell Laboratories, Holmdel, NJ 07733

MASAHIKO HAYASHI and KAZUYOSHI SUNADA: Department of Astronomy, University of Tokyo, Bunkyo-ku, Tokyo 113, Japan

MARK HERELD: Department of Astronomy and Astrophysics, University of Chicago, Chicago, IL 60637

NAOMI HIRANO and OSAMU KAMEYA: Nobeyama Radio Observatory, National Astronomical Observatory, Minamimaki, Nagano 384-13, Japan

FRANK ISRAEL: Sterrewacht/Huygens Laboratory, Wassenaarsweg 78, 2333 AL Leiden, Netherlands

MARC W. POUND: HOH L-222, AT&T Bell Laboratories, Holmdel, NJ 07733

ANTONY A. STARK: HOH L-231, AT&T Bell Laboratories, Holmdel, NJ 07733

HARLEY THRONSON, JR.: Department of Physics and Astronomy, University of Wyoming, University Station, Box 3905, Laramie, WY 82071

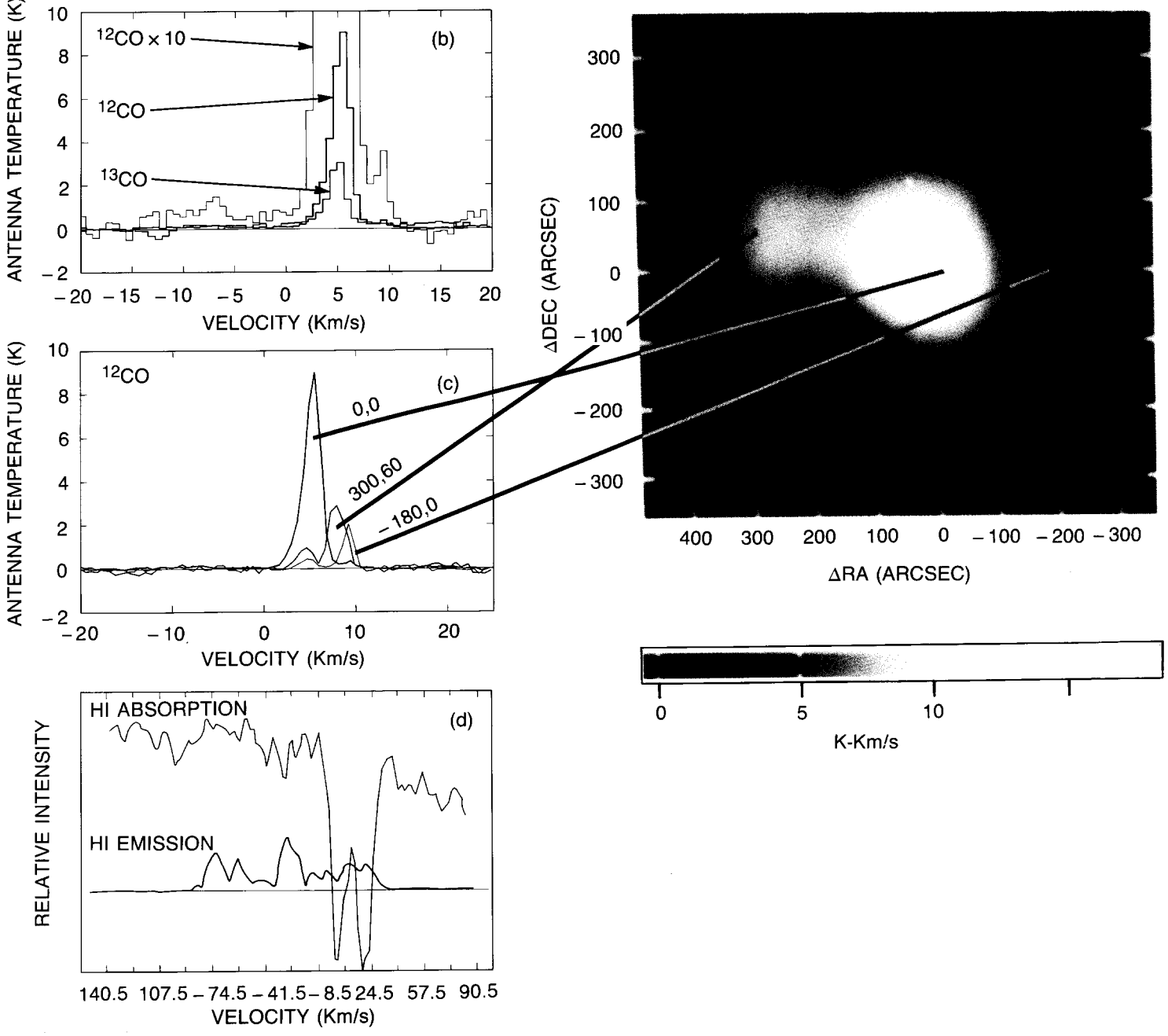


FIG. 1.—(*a*) Gray-scale map (7 m) of G70.7 + 1.2 showing $^{12}$CO integrated line intensity $\int T_A^*(V)dV$ between 1 and 11 km s$^{-1}$. (*b*) Seven meter spectra of the CO line toward the core of G70.7 + 1.2. $^{12}$CO (*bold*) and $^{12}$CO magnified 10 times (*thin*), showing the faint line wings which may be due to gas accelerated by the interaction of the radio bubble with the globule, and $^{13}$CO emission from the core (intermediate thickness). (*c*) Seven meter spectra of the CO line toward the core of G70.7 + 1.2. $^{12}$CO showing the three cloud components centered at (0, 0) (arcminute offsets) in the bold line, (5, 1) in the intermediate line, and (−3, 0) in the thin line. (Note that the offsets are in arcseconds in the figure.) The (0, 0) coordinates in all figures refer to $\alpha(1950) = 20^h02^m27^s.5$, $\delta(1950) = 33°30'30''$. (*d*) Westerbork H I spectra. H I absorption was measured on 1–3 km baselines while the emission was measured on a 36 m baseline. The intensity scale is uncalibrated.

1989ApJ...338L..65B



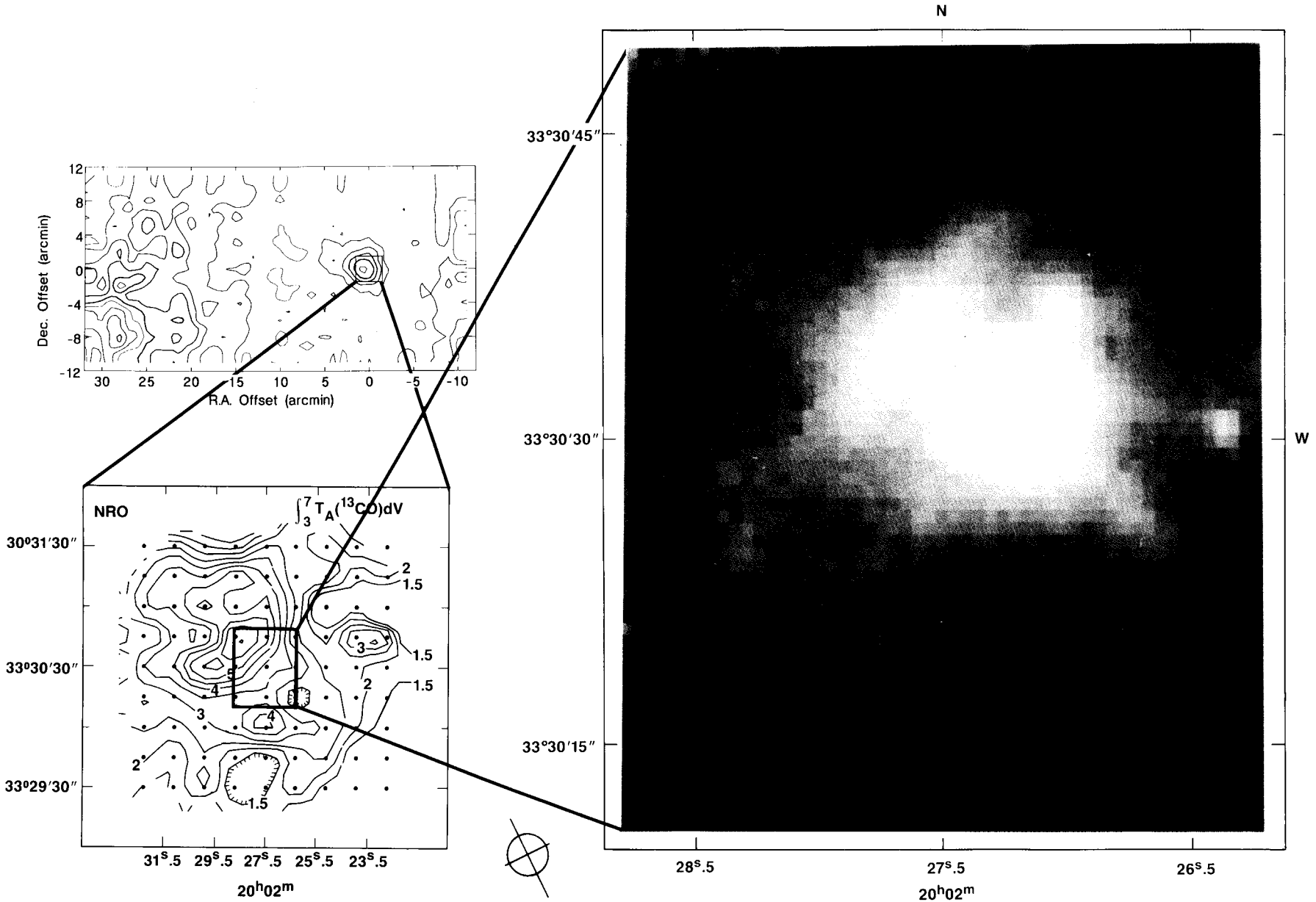


FIG. 2.—(*a*) (*upper left*) A $^{13}$CO map (7 m) showing the integrated line intensity $\int T_A^*(V)dV$ between 0 and 12 km s$^{-1}$ in 1 K km s$^{-1}$ steps. (*b*) (*lower left*) The Nobeyama $^{13}$CO map with contours showing $\int T_A(V)dV$ integrated from 3 to 7 km s$^{-1}$ which includes 90% of the emission. Levels are labeled on the map in units of K km s$^{-1}$. Note that the levels are in $T_A$ and *not* $T_A^*$. The Nobeyama map intensity scale has to be multiplied by a factor of order 2 to correct for the antenna primary beam efficiency. ($\eta_{\rm Bell} \approx 90\%$ while $\eta_{\rm NRO} \approx 40\%$.) (*c*) An infrared image of the G70.7 + 1.2 region in the 2.2 $\mu$m window with a scale of 0.″605 per pixel. The features seen at 45° are diffraction spikes. The relative sizes of each component of this plate are indicated by the boxes.

1989ApJ...338L..65B



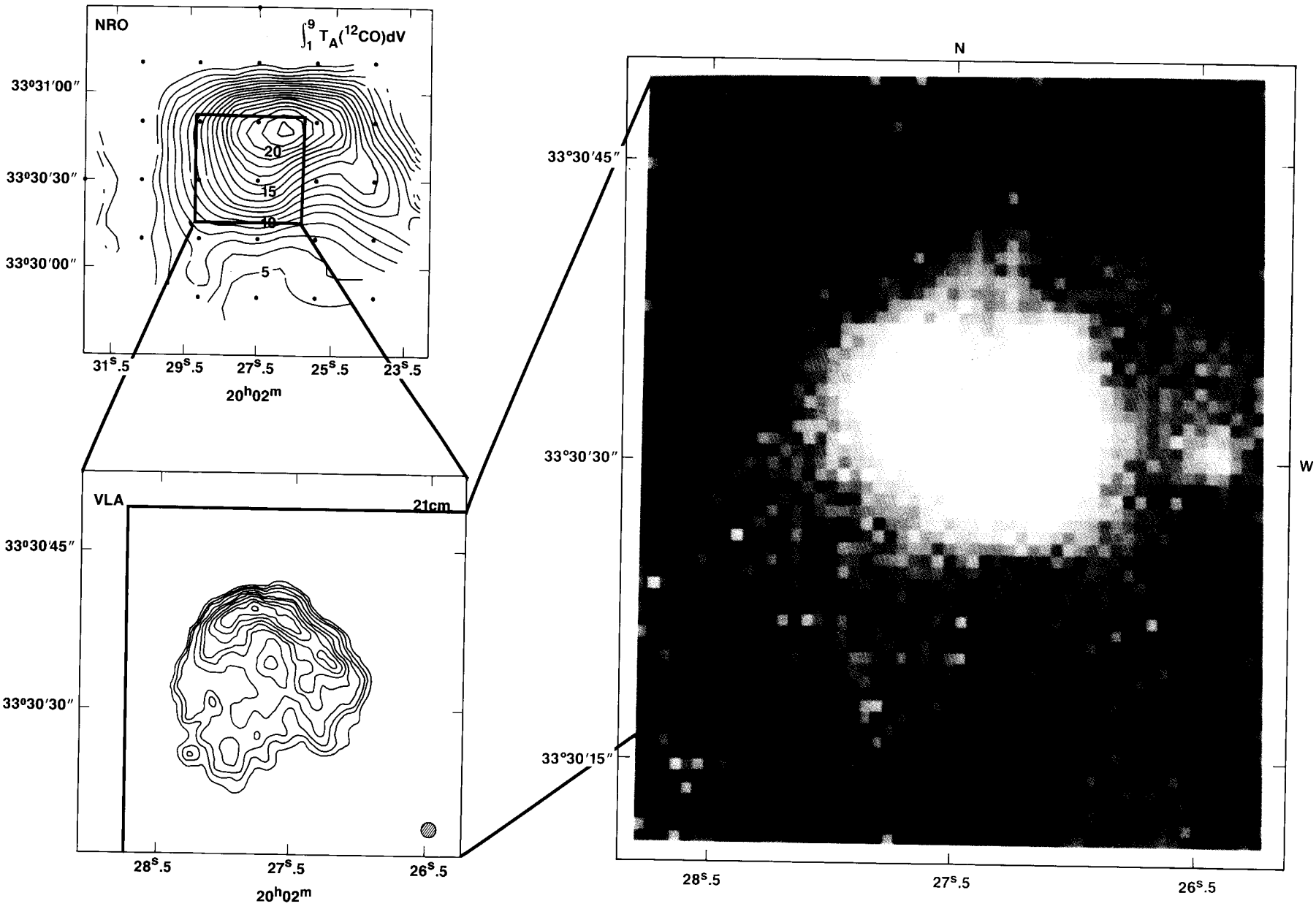


FIG. 3.—(*a*) (*upper left*) The Nobeyama $^{12}$CO map with contours showing $\int T_A(V)dV$ integrated from 1 to 9 km s$^{-1}$ which includes 95% of the emission. Levels are labeled on the map in units of K km s$^{-1}$. Note that as in Fig. 1, the levels are in $T_A$ and *not* $T_A$*. There was a substantial pointing drift during the 2 hr period in which the $^{12}$CO Nobeyama data were obtained, so the absolute position of the map may be in error by as much as 15″. (*b*) A 21 cm continuum map taken from de Muizon *et al.* (1988). (*c*) An infrared image of the G70.7 + 1.2 region in the 1.6 μm window with a scale of 0.″605 per pixel. The features seen at 45° are diffraction spikes. The relative sizes of each component of this figure are indicated by the boxes.